Scanning Tunneling Microscopy of a Luttinger Liquid

Sebastian Eggert
Institute of Theoretical Physics, Chalmers University of Technology and Göteborg University, S-412 96 Göteborg, Sweden
(Received 2 August 1999)

Explicit predictions for scanning tunneling microscopy (STM) on interacting one-dimensional electron systems are made using the Luttinger liquid formalism. The STM current changes with the distance from an impurity or boundary in a characteristic way, which reveals the spin-charge separation and the interaction strength in the system. The current exhibits Friedel-like oscillations, but also carries additional modulated behavior as a function of voltage and distance, which shows the spin-charge separation in real space. Moreover, very close to the boundary the current is strongly reduced, which is an indication of the interaction strength in the system.

PACS numbers: 71.10.Pm, 61.16.Ch, 71.27.+a, 73.40.Gk

In the past two decades the interest in quasi-one-dimensional physics has been spurred by experimental progress in constructing smaller and more refined structures such as carbon nanotubes, atomic point contacts, and mesoscopic quantum wires produced by etching [1] or cleaved edge overgrowth [2]. More recently it was even possible to produce single atomic chains by depositing gold on a silicon surface [3].

The theoretical foundation for describing interacting one-dimensional electrons was laid in the early 80's with the concept of a Luttinger liquid (LL) [4]. Interestingly, the electron-electron interactions cannot ever be neglected in one dimension which makes those systems fundamentally non-Fermi-liquid-like. The elementary excitations are described by separate spin and charge quasiparticles which move at different velocities [5]. The correlation functions are power laws with exponents that are related to a single interaction constant g.

Angle resolved photoemission experiments have made some progress in identifying a possible signature of spin-charge separation in quasi-one-dimensional compounds [3,6]. On the other hand, in mesoscopic wires most experiments focus on conductivity measurements [1,2]. However, from those experiments it is very difficult to extract information about the fundamental interactions within the wire. To test the important theoretical concept of spin-charge separation in mesoscopic systems, other methods must be considered.

One difficulty in producing a good wire is the fact that even small impurity perturbations effectively cut the wire at low temperatures [7]. However, such boundaries give rise to other interesting effects, which can even reveal the LL behavior as we will show below. One well-known impurity effect in metals is the induced charge density fluctuation at twice Fermi wave vector, the so-called Friedel oscillation. In the case of carbon nanotubes, the Friedel oscillations have already been used to show the more complicated electronic structure [8], which stems from a rolled up two-dimensional graphite sheet.

We now make predictions for a scanning tunneling microscopy (STM) experiment along a simple quantum wire described by the LL model with an open end instead of leads, i.e., electrons which have been confined to move in one dimension by clever gating or an appropriate deposit on a surface. We show that the spatial structure of the tunneling current reveals both the spin-charge separation and the interaction strength in the LL system.

The STM current I is directly related to how many electron states are locally available in the LL system and in the tunneling tip. In particular, at position r and for a given tunneling voltage V, we can write

$$I(V,r) \propto \int_0^V d\omega\, N(\omega,r) f(\omega - V), \qquad (1)$$

where $N(\omega,r)$ is the local density of states (DOS) in the LL with ω measured relative to the Fermi energy, and f is the DOS in the tip. We do not know the detailed properties of the tip, but we can assume that $f(\omega)$ is smooth compared to the more singular structure of $N(\omega)$, so that $f = \text{const}$ is a valid approximation. The DOS of the system is given in terms of the time-time correlation functions in the LL at position r:

$$N(\omega,r) \equiv \frac{1}{2\pi} \int_{-\infty}^{\infty} e^{i\omega t} \langle \{\Psi_\sigma(r,t), \Psi_\sigma^\dagger(r,0)\} \rangle\, dt\,, \qquad (2)$$

where ω is measured relative to the Fermi energy. It is already well understood how to calculate the DOS as a function of energy ω with the LL formalism [5,9], but as described in this Letter it is the spatial structure as a function of distance r from a boundary that also explicitly shows the spin-charge separation.

The LL Hamiltonian describes one-dimensional electrons with short range interactions in the low-temperature limit below some energy cutoff Λ. In that limit, the dispersion is approximately linear and the electron-electron scattering rate can be taken as momentum independent. The high energy cutoff Λ is large compared to the temperature, but about one magnitude less than the bandwidth for typical lattice models. The electron field $\Psi_\sigma(x)$ is expressed in terms of left- and right-moving Fermions at the Fermi points $\pm k_F$:

$$\Psi_\sigma(x) = e^{-ik_F x}\psi_L^\sigma(x) + e^{ik_F x}\psi_R^\sigma(x). \quad (3)$$

We also define the Fermion currents $J_{L/R}^\sigma \equiv :\psi_{L/R}^{\sigma\dagger}\psi_{L/R}^\sigma:$. Umklapp scattering is suppressed away from half filling, and remarkably all forward scattering processes can be described by expressing the spin and charge currents in terms of separate bosonic variables ϕ_c and ϕ_s and their conjugate momenta Π_c and Π_s:

$$J_L^{c/s} \equiv \tfrac{1}{\sqrt{2}}(J_L^\uparrow \pm J_L^\downarrow) = \tfrac{1}{\sqrt{4\pi}}(\Pi_{c/s} + \partial_x\phi_{c/s}). \quad (4)$$

The LL Hamiltonian density is then written as

$$\mathcal{H} = \tfrac{v_c}{2}[g^{-1}(\partial_x\phi_c)^2 + g\Pi_c^2] + \tfrac{v_s}{2}[(\partial_x\phi_s)^2 + \Pi_s^2], \quad (5)$$

which describes two independent bosonic excitations for spin and charge separately. Because of SU(2) invariance the spin boson is a free field, but the charge boson gets rescaled by the LL parameter g which is less than unity for repulsive interactions.

After the linearization around the Fermi points in Eq. (3), we can write (omitting the spin indices σ)

$$\begin{aligned}\langle\Psi(r,t)\Psi^\dagger(r,0)\rangle = {} & \langle\psi_L(r,t)\psi_L^\dagger(r,0)\rangle + \langle\psi_R(r,t)\psi_R^\dagger(r,0)\rangle \\ & + e^{i2k_F r}\langle\psi_R(r,t)\psi_L^\dagger(r,0)\rangle \\ & + e^{-i2k_F r}\langle\psi_L(r,t)\psi_R^\dagger(r,0)\rangle. \quad (6)\end{aligned}$$

The last two terms carry a rapid oscillation with twice the Fermi wave vector $2k_F r$ reminiscent of Friedel oscillations, while the first two terms are slowly varying. The tunneling current in Eq. (1) therefore has a rapidly oscillating Friedel part $I_{\rm osc}$ and a uniform part $I_{\rm uni}$ with a spatial dependence that is smooth compared to $e^{i2k_F r}$:

$$I(V,r) = I_{\rm uni}(V,r) + \cos(2k_F r + \phi) I_{\rm osc}(V,r). \quad (7)$$

In a translational invariant system, the left and right movers are uncorrelated $\langle\psi_L\psi_R^\dagger\rangle = 0$ and we cannot observe any spatial structure. A generic impurity, however, scatters left movers into right movers and the resulting correlation functions depend on the distance r from the end. Such boundary correlation functions have first been calculated for the spin channel [10] and later also for the full electron field [11–13]. We consider an open boundary at the origin $r = 0$ of a relatively long system so that $N(\omega)$ is continuous (the other end of the system is far away and can be neglected for now). In that case we find the following for the uniform terms:

$$\begin{aligned}\langle\psi_L(r,t)\psi_L^\dagger(r,0)\rangle \propto {} & \left[\frac{1}{\alpha + iv_s t}\right]^{1/2}\left[\frac{1}{\alpha + iv_c t}\right]^{a+b} \\ & \times\left[\frac{4r^2}{(\alpha + iv_c t)^2 + 4r^2}\right]^c, \quad (8)\end{aligned}$$

and for the Friedel terms

$$\langle\psi_R(r,t)\psi_L^\dagger(r,0)\rangle \propto \left[\frac{1}{\alpha + i(v_s t - 2r)}\right]^{1/2}\left[\frac{1}{\alpha + i(v_c t - 2r)}\right]^{a}\left[\frac{1}{\alpha + i(v_c t + 2r)}\right]^{b}\left[\frac{|2r|}{\alpha + iv_c t}\right]^{2c}, \quad (9)$$

where the exponents are given in terms of the interaction parameter g:

$$a = (\tfrac{1}{g} + g + 2)/8, \qquad b = (\tfrac{1}{g} + g - 2)/8,$$
$$c = (\tfrac{1}{g} - g)/8.$$

The short distance cutoff $\alpha \sim v/\Lambda$ is small compared to all other length scales in the system, and we take $\alpha \to 0^+$ in all following calculations. The corresponding expressions for left and right movers exchanged can be obtained by taking $r \to -r$.

Let us first consider the uniform part of the current $I_{\rm uni}$ as determined by the analytic structure of Eq. (8). A change of variables $t' = t/r$ in Eq. (2) and $\omega' = r\omega$ in Eq. (1) shows that the uniform current $I_{\rm uni}$ is a function of the scaling variable rV:

$$I_{\rm uni}(V,r) = r^{-(1/g+g+2)/4}F(rV), \quad (10)$$

For noninteracting electrons ($g = 1, v_c = v_s = v$) we get $a = \frac{1}{2}, b = c = 0$ corresponding to a single pole of order one at $t = i\alpha$ in Eq. (8). The integration in Eq. (2) gives a constant from the residue in the upper half plane; i.e., the DOS is independent of r and ω, and Eq. (1) simply gives $I_{\rm uni} \propto V$ for noninteracting electrons. However, even for small interactions the single pole splits into three singularities at $t = i\alpha$ and $t = \pm 2r/v_c + i\alpha$ in Eq. (8). Close to the boundary the behavior of the Fourier transform in Eq. (2) is then dictated by the large time behavior of Eq. (8) and we find

$$I_{\rm uni} \propto r^{(1/g-g)/4}V^{(1/g+1)/2} \quad \text{for } r < v_c/V, \quad (11)$$

i.e., a characteristic depletion as $r \to 0$ for repulsive interactions $g < 1$. On the other hand, far away from the boundary $r \gg v_c/V$ the behavior is dominated by the most divergent singularity and we find

$$I_{\rm uni} \propto V^{(1/g+g+2)/4} \quad \text{for } r > v_c/V, \quad (12)$$

which is largely independent of r. However, the integration of the deformed contour in Eq. (2) around the branch cuts of the weaker singularities also contributes, multiplied by a corresponding slowly oscillating "residue factor" $e^{\pm 2ir\omega/v_c}$. This results in an additional slowly oscillating contribution with $\cos(2rV/v_c)$ that drops off with $r^{(1/g-g-8)/8}$. The depletion with the slow oscillations towards a constant current is depicted in Fig. 1 for $g = 3/4$ from doing the integrals numerically. None of the singularities in Eq. (8) depend on the spin velocity v_s and

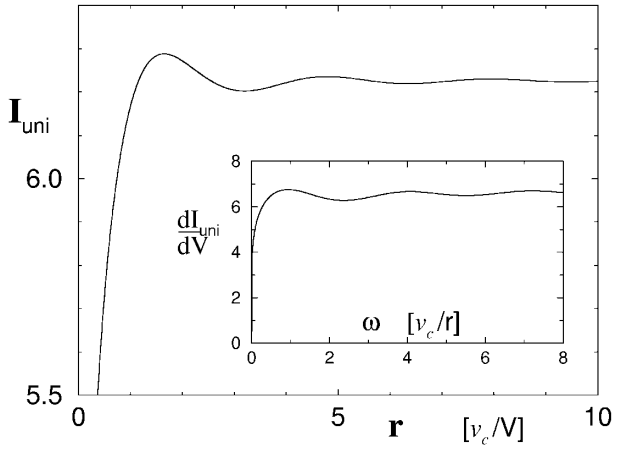

FIG. 1. The uniform current $I_{\rm uni}$ in arbitrary units as a function of r for $g = 3/4$. The inset shows $dI_{\rm uni}/dV$ as a function of ω at a position r.

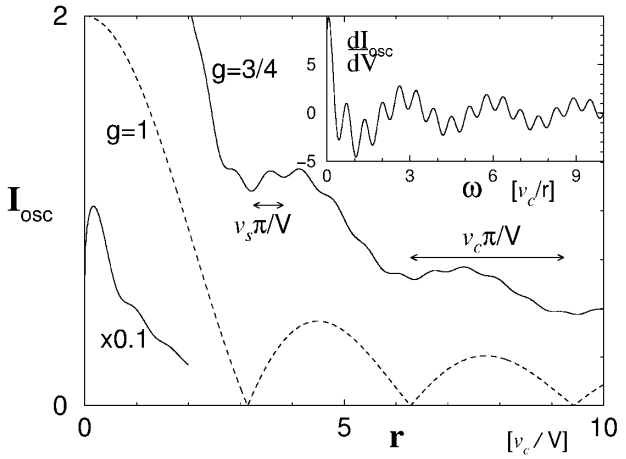

FIG. 2. The Friedel amplitude of the tunneling current in arbitrary units as a function of r for $g = 1$ and $g = 3/4$, $v_c/v_s = 5$. The inset shows $dI_{\rm osc}/dV$ at a position r with an arbitrarily chosen phase $e^{i2k_F r} = 1$.

therefore the uniform current $I_{\rm uni}$ will *not* show any signs of spin-charge separation. Nonetheless, the weaker singularities still give the characteristic slowly oscillating structure due to interactions.

The effect of the last two "Friedel" terms in Eq. (6), on the other hand, will reveal the spin-charge separation. The amplitude $I_{\rm osc}$ of the rapidly oscillating Friedel current has the same scaling form as in Eq. (10) but with an even richer behavior for F. Already for noninteracting electrons we find a single pole at $t = 2r/v + i\alpha$ in Eq. (9) which results in $N(\omega, r) \propto \cos(2k_F r + 2r\omega/v)$. The integration in Eq. (1) gives a strong r dependence of the amplitude $I_{\rm osc} \propto \sin(\frac{rV}{v})/r$ ("amplitude modulation") as shown in Fig. 2 for $g = 1$. With interactions we now find four different singularities at $t = i\alpha, t = \pm 2r/v_c + i\alpha$, and $t = 2r/v_s + i\alpha$ in Eq. (9). The long-time behavior of Eq. (9) is the same as for the uniform terms in Eq. (8), so that we get the same universal depletion for $I_{\rm osc}$ as in Eq. (11) very close to the boundary $r < v_s/V$. For larger distances from the boundary $r \gg v_c/V$, however, the dropoff of the Friedel current is determined by the leading singularity in Eq. (9)

$$I_{\rm osc} \propto \begin{cases} r^{-(1/g+g+2)/8} V^{(1/g+g+2)/8}, & \frac{1}{3} < g < 1 \\ r^{-(1+g)/2} V^{(1/g-g)/4}, & g < \frac{1}{3} \end{cases} . \tag{13}$$

More importantly, the Friedel amplitude $I_{\rm osc}$ has an oscillating superstructure from the residue factor of each singularity. The strong amplitude modulation with $\sin \frac{rV}{v}$ has already been demonstrated for the noninteracting case, but the ratio of the velocities v_c/v_s can now be much larger than one. Therefore, we observe two separate spin and charge amplitude modulations of $I_{\rm osc}$ with rV/v_s and with rV/v_c, respectively (which are still smooth compared to the overall oscillation of $2k_F r$). This behavior is demonstrated in Fig. 2 for $g = 3/4$ and $v_c/v_s = 5$. The physical interpretation is that we observe the superposition of all electron wave functions in the energy range from 0 to V which exhibits the spin-charge separation due to the interference from the boundary.

We have shown that the spatial electronic structure of an LL indeed shows the signatures of the spin-charge separation, but it is important to critically analyze to what extent this could be observed in a realistic STM experiment. As an example, we consider the monatomic gold chains on a slanted silicon surface Si(111)-Au(5×1), which showed the signature of LL behavior in photoemission experiments [3]. The spin-charge separation seems to be present for all excitations over the entire bandwidth (ca. 1 eV), but, to observe the particular STM structures that we predict here, the voltage has to be below the cutoff Λ which is about 0.1 eV for this system. The most easily observable feature in an STM experiment is probably the depletion of the tunneling current as a function of distance near the boundary. The range of this depletion is given by $r \approx v_F/V$, where $v_F \approx 6 \times 10^5$ m/s for the gold chains, so that for $V < 100$ meV the range is at least $r \gtrsim 40$ Å. Already from the shape of this depletion an approximate estimate of g can be made from Eq. (11). Second, it is important to analyze the Friedel oscillations, which is a more difficult task. For the gold chains the Fermi vector is $k_F = \pi/2a$ with an interatomic spacing of $a = 3.83$ Å, so that the $2k_F r$ oscillations are commensurate with the lattice. This makes the Friedel oscillations easier to detect, but the small amplitude modulations in Fig. 2 may not show up very clearly. The Friedel amplitude is modulated by at most 30% by the charge waves, while the spin modulations are even smaller. The spin modulations are actually *weaker* for stronger interactions (about 10% for $g \sim 1$, but only 1% for $g < 1/2$). Nonetheless, even if only a small hint of those superstructures shows up in an STM image, it should be possible to track those modulations for different voltages. This will change their period systematically and may make it possible to identify them unambiguously.

Interestingly, the total modulation is much *stronger* without any spin-charge separation ($g = 1$), so if it cannot be observed at all it would also be an indication of interaction effects. For larger voltages $V > \Lambda$ it is more instructive to look at the total density of electrons given directly by Eqs. (8) and (9) in the limit $t \to 0$, which recovers the established dropoff of the Friedel terms with $r^{-(1+g)/2}$ [11,14], but without any spin-charge modulations.

The measurement of dI/dV as a function of voltage in an STM experiment (spectral mode) will give additional information about the local DOS. Close to the boundary dI/dV has considerable structure as indicated in the insets of Figs. 1 and 2. The additional contribution $dI_{\rm osc}/dV$ from the Friedel terms in Fig. 2 is smaller and depends on the choice of phase $e^{i2k_F r}$, but shows the separate spin-charge effects very clearly. The gold chains mentioned above showed a surprisingly strong depletion of the spectral weight at the Fermi surface as a function of energy in photoemission experiments [3]. It would be interesting to see if STM experiments on the very same samples also show such a strong depletion of the DOS with a characteristic power law V^{2b}.

One approximation we made is that the DOS in the tip $f(\omega)$ is relatively smooth, which is not too restrictive since the observed structures in Figs. 1 and 2 can be reproduced for almost all forms of $f(\omega)$ as long as there is a sharp upper limit at V in the integral of Eq. (1). It is also possible to average over both signs of the voltage to eliminate the DOS of the tip somewhat, since the anticommutator in Eq. (2) gives the same singularities for $t \to -t$; i.e., $N(\omega) = N(-\omega)$.

The distance from the tip to the sample is also important, since the tip may influence the system and play the role of an impurity itself. The optimal distance can be determined in the actual experiment by operating in spectral mode somewhere in the bulk of the wire. If the dI/dV curve changes qualitatively as the tip-sample distance is decreased (except for an overall scale), then this would be a clear sign that the tip influences the sample. In particular, if the tip starts to act as an impurity the dI/dV curve should show a stronger depletion with the power law $V^{(1/g-1)/2}$ as $V \to 0$.

So far we have considered only a perfectly reflecting impurity, because it is expected that any generic perturbation renormalizes to the open boundary fixed point [7]. However, in an intermediate range around a "weaker" impurity the Friedel effects show a nonuniversal behavior described in terms of a form factor [14]. The range of this so-called boundary layer shrinks to zero for a perfectly reflecting barrier. Also interesting are "active" impurities that have a net magnetic moment or carry an electric charge. In the presence of interactions those impurities may be overscreened; i.e., the nearest electrons overcompensate for the impurity charge or spin and in turn get screened by the next-nearest neighbors, etc. This finally results in a screening cloud which is also a $2k_F r$ effect, since the impurity Hamiltonian $H_{\rm imp}$ induces a nonzero expectation value in the Friedel terms of Eq. (6); i.e., $\langle \psi_L \psi_R^\dagger H_{\rm imp} \rangle \neq 0$. The presence of both backscattered and induced Friedel terms has recently been demonstrated for a two-channel Kondo impurity [15].

Finally, we must also consider the effect of a second boundary in a finite system at $r = L$. The correlation functions in Eqs. (8) and (9) are then described by powers of sine functions $\sin \frac{\pi v t}{2L}$ [11,13]. We expect that the spatial structure from the interference of the standing waves gives a similar picture as in Figs. 1 and 2 close to the boundaries as long as $V \gg \pi v/L$. However, a more dramatic finite size effect is a discrete spectrum $N(\omega)$ due to the appearance of δ functions in Eq. (2). This results in Coulomb-blockade-like charging steps in $I(V)$, which can also reveal the spin-charge separation and the interaction strength in the LL [13].

In conclusion, we have shown that the tunneling current has decaying Friedel-like oscillations in a range around a boundary, but additionally the Friedel amplitude carries a characteristic periodic modulation in real space which reveals the separate spin and charge parts of the electron wave functions. The period of those modulations is a function of the tunneling voltage, which is assumed to be small. We also find a characteristic depletion very close to the boundary of both the Friedel current and the uniform current, which is immediately related to the interaction constant in the wire.

The author is very grateful to Henrik Johannesson for inspirational discussions and to Yves Baer for an early copy of Ref. [3]. This research was supported by the Swedish Natural Science Research Council with Grants No. F-AA/FU 12288-301 and No. S-AA/FO 12288-302.

[1] S. Tarucha *et al.*, Solid State Commun. **94**, 413 (1995).
[2] A. Yacoby *et al.*, Phys. Rev. Lett. **77**, 4612 (1996).
[3] P. Segovia *et al.*, Nature (London) **402**, 504 (1999).
[4] F. D. M. Haldane, J. Phys. C **14**, 2585 (1981).
[5] For a review, see J. Voit, Rep. Prog. Phys. **58**, 977 (1995).
[6] C. Kim *et al.*, Phys. Rev. Lett. **77**, 4054 (1996).
[7] C. L. Kane and M. P. A. Fisher, Phys. Rev. B **46**, 7268 (1992).
[8] C. L. Kane and E. J. Mele, Phys. Rev. B **59**, 12 759 (1999); W. Clauss *et al.*, Europhys. Lett. **47**, 601 (1999).
[9] K. Schönhammer and V. Meden, Phys. Rev. B **47**, 16 205 (1993); J. Voit, J. Phys. Condens. Matter **5**, 8305 (1993).
[10] S. Eggert and I. Affleck, Phys. Rev. B **46**, 10 866 (1992); Phys. Rev. Lett. **75**, 934 (1995).
[11] M. Fabrizio and A. O. Gogolin, Phys. Rev. B **51**, 17 827 (1995).
[12] S. Eggert *et al.*, Phys. Rev. Lett. **76**, 1505 (1996).
[13] A. E. Mattsson *et al.*, Phys. Rev. B **56**, 15 615 (1997); S. Eggert *et al.*, Phys. Rev. B **56**, R15 537 (1997).
[14] R. Egger and H. Grabert, Phys. Rev. Lett. **75**, 3505 (1995); A. Leclair *et al.*, Phys. Rev. B **54**, 13 597 (1996).
[15] S. Eggert and S. Rommer, Phys. Rev. Lett. **81**, 1690 (1998); Physica (Amsterdam) **261B**, 200 (1999).